

See discussions, stats, and author profiles for this publication at: <https://www.researchgate.net/publication/273463370>

Luciferin and derivatives as a DYRK selective scaffold for the design of protein kinase inhibitors

ARTICLE *in* EUROPEAN JOURNAL OF MEDICINAL CHEMISTRY · FEBRUARY 2015

Impact Factor: 3.45 · DOI: 10.1016/j.ejmech.2015.02.035 · Source: PubMed

CITATION

1

READS

75

6 AUTHORS, INCLUDING:



[Ulli Rothweiler](#)

University of Tromsøe

14 PUBLICATIONS 266 CITATIONS

[SEE PROFILE](#)



[Wenche Stensen](#)

University of Tromsøe

27 PUBLICATIONS 776 CITATIONS

[SEE PROFILE](#)



[Richard Alan Engh](#)

University of Tromsøe

108 PUBLICATIONS 6,738 CITATIONS

[SEE PROFILE](#)



[John Sigurd Svendsen](#)

University of Tromsøe

92 PUBLICATIONS 2,880 CITATIONS

[SEE PROFILE](#)



Contents lists available at ScienceDirect

European Journal of Medicinal Chemistry

journal homepage: <http://www.elsevier.com/locate/ejmech>

Original article

Luciferin and derivatives as a DYRK selective scaffold for the design of protein kinase inhibitors



Ulli Rothweiler^a, Jonas Eriksson^{b,1}, Wenche Stensen^{b,c}, Frederick Leeson^{b,c},
Richard A. Engh^{a,**}, John S. Svendsen^{b,c,*}

^a The Norwegian Structural Biology Centre, Department of Chemistry, UiT The Arctic University of Norway, N-9037 Tromsø, Norway

^b Lytix Biopharma AS, P.O. Box 6447, Tromsø Science Park, N-9294 Tromsø, Norway

^c Department of Chemistry, UiT The Arctic University of Norway, N-9037 Tromsø, Norway

ARTICLE INFO

Article history:

Received 19 December 2014

Received in revised form

19 January 2015

Accepted 19 February 2015

Available online 25 February 2015

Keywords:

Luciferin

Protein kinase

Inhibitor profiling

Drug design

Crystallography

ABSTRACT

D-Luciferin is widely used as a substrate in luciferase catalysed bioluminescence assays for *in vitro* studies. However, little is known about cross reactivity and potential interference of D-luciferin with other enzymes. We serendipitously found that firefly luciferin inhibited the CDK2/Cyclin A protein kinase. Inhibition profiling of D-luciferin over a 103-protein kinase panel showed significant inhibition of a small set of protein kinases, in particular the DYRK-family, but also other members of the CMGC-group, including ERK8 and CK2. Inhibition profiling on a 16-member focused library derived from D-luciferin confirms that D-luciferin represents a DYRK-selective chemotype of fragment-like molecular weight. Thus, observation of its inhibitory activity and the initial SAR information reported here promise to be useful for further design of protein kinase inhibitors with related scaffolds.

© 2015 Elsevier Masson SAS. All rights reserved.

1. Introduction

Novel compounds with protein kinase inhibitory properties may be highly valuable, and screening for such activity is therefore included in many bioprospecting efforts. The kinase RR [1] technology ("Reaction Rate") is a popular choice to identify fractions with protein kinase inhibitory activity; it was developed to enable real-time monitoring target peptide/protein phosphorylation by protein kinases [2]. In this assay, luciferase and D-luciferin are present during the entire kinase reaction, allowing continuous measurement of light emission, although for high throughput screening, measurement of light emission is required only at the beginning and after a pre-set time point. In the late evaluation process prior to the launch of Kinase RR, the assay was tested

against a panel of 38 protein kinases selected to represent active site diversity. Although Kinase RR performed well and could be consistent against a reference assay method, there was one protein kinase that repeatedly failed; casein kinase 2 (CK2). During the Kinase RR implementation in a bioprospecting screen, a similar failure was found for CDK2/Cyclin A. The reason for this failure could be attributed to be the direct inhibitory action of D-luciferin on the CDK2/Cyclin A complex. The finding that many protein kinases are unaffected by luciferin while a few kinases are inhibited by the compound prompted us to investigate whether D-luciferin inhibited additional protein kinases, and whether D-luciferin could serve as a scaffold for the construction of novel selective protein kinase inhibitors, by preparing a luciferin derived focused library and profiling this library against a large protein kinase panel.

2. Results

2.1. Preparation of inhibitors and protein kinase activity studies

Kinase profiling assays of D-luciferin (**1**) at a concentration of 100 μ M were performed with a 103-kinase panel at the International Centre for Kinase Profiling at the University of Dundee, UK [3]. The profile revealed that 21 kinases were inhibited significantly

* Corresponding author. Lytix Biopharma AS, P.O. Box 6447, Tromsø Science Park, N-9294 Tromsø, Norway.

** Corresponding author.

E-mail addresses: richard.ENGH@uit.no (R.A. Engh), john-sigurd.svendsen@uit.no (J.S. Svendsen).

¹ Present address: Laboratories for Chemical Biology Umeå (LCBU), Chemical Biology Consortium Sweden (CBCS), Department of Chemistry, Umeå University, SE-901 87 Umeå, Sweden.

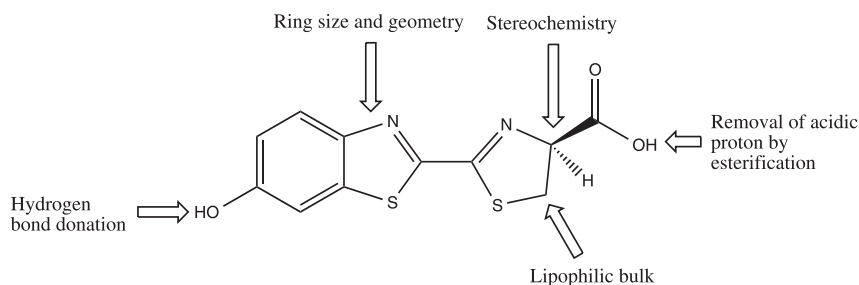


Fig. 1. SAR variations applied to the D-luciferin scaffold.

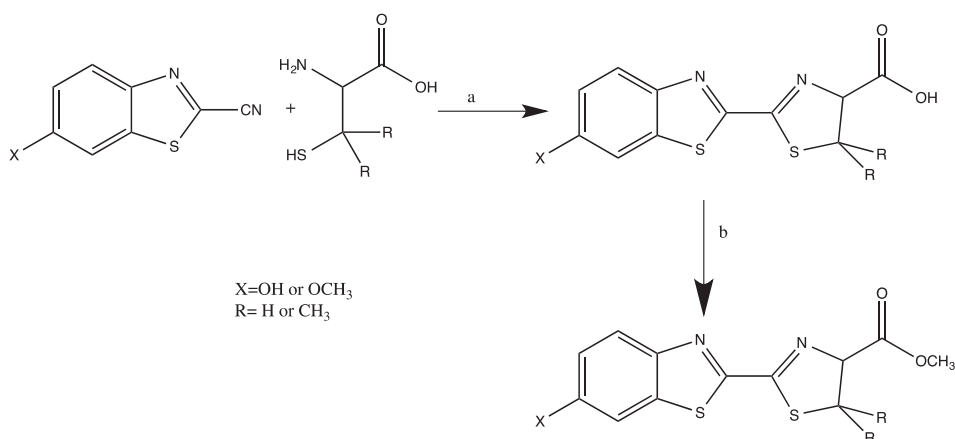
($\leq 25\%$ remaining activity) by D-luciferin, but also that the majority of kinases were unaffected even at this relatively high concentration. Among the most luciferin sensitive kinases were the DYRK family (1a, 2 and 3 tested), Auroras B and A, CK2, PKB β , VEGFR1, GCK, RSK2, ERK8 and PIM3. The discovery that several kinases of potential interest as drug targets were inhibited by D-luciferin prompted us to prepare an exploratory structure–activity relationship (SAR) study on D-luciferin as a scaffold for design of kinase inhibitors (Fig. 1).

The SAR-library design was based on the assumption that the functional groups, i.e. the phenolic hydroxyl group on the benzothiazole ring system and the carboxylic acid on the dihydrothiazole ring of luciferin, were important for binding interactions with the affected kinases. These groups were substituted by methyl ether and methyl ester derivatives, respectively. Further variations included the replacement of the bicyclic benzothiazole by a quinoline, position of the hydroxyl group on the quinoline ring, the introduction of methyl groups in the dihydrothiazole ring, and the absolute configuration of the carboxylic acid substituent of the dihydrothiazole ring. The benzothiazole and quinoline SAR-libraries were prepared in the conventional manner as outlined in Scheme 1 (following White [4]) by condensing a 2-cyanobenzothiazole (or a 2-cyanoquinoline) with (*R*)- or (*S*)-cysteine (or (*R*)- or (*S*)-penicillamine), with subsequent esterification of the carboxylic acid where necessary. This method is used in nearly all preparations of lucifeins today [5]. The advantage of condensing cysteine derivatives with cyanobenzothiazoles or cyanoquinolines at a late stage in the process is that the process is mild, produces high yields and preserves the stereocenter of the cysteine derivative in the dihydrothiazole ring [5]. The preparative chemistry of D-luciferin has been recently reviewed [6].

The phenols, 6-hydroxy-1,3-benzothiazole-2-carbonitrile and 6-hydroxyquinoline-2-carbonitrile, were prepared from their corresponding commercially available methyl ethers by treatment with dry pyridinium chloride at 200 °C [7]. The individual members of this SAR-library are presented in Table 1.

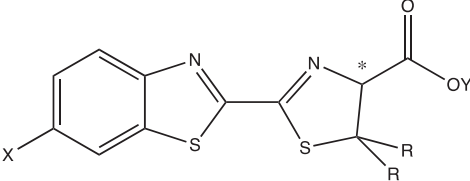
2.2. Kinome profiling analysis

Finally, the remaining 15 members of the SAR-library were subjected to kinase inhibition profiling using the same 103-kinase panel. All assays were performed with an ATP concentration at or below Km for the particular protein kinase. The complete results from the kinome profiling measured as per cent remaining protein kinase activity at a 100 μ M inhibitor concentration are given in the Supplementary information (SI) section, and the inhibitory activity against a selected set of kinases is presented in Table 1. Strong inhibition was defined as $< 15\%$ remaining activity, and significant inhibition was defined as being in the range of 16–25% remaining activity. The Table in SI is sorted according to the average of the remaining activities for a particular protein kinase over all 16 compounds in the luciferin library. The protein kinases on the top of the Table are thus protein kinases that are strongly inhibited by many members of the luciferin library. The protein kinase that is most strongly inhibited across the luciferin library is DYRK2, with an average residual activity of less than 13%. The two other DYRK family kinases represented in the profiling set, DYRK1a and DYRK3, follow next on the list. PIM3, ERK8 and CK2 are three non-DYRK protein kinases that are strongly inhibited by many compounds in the luciferin library. Following these six kinases, the inhibition either becomes weaker or more irregular. Aurora B is also strongly inhibited by a few compounds in the library, but is virtually

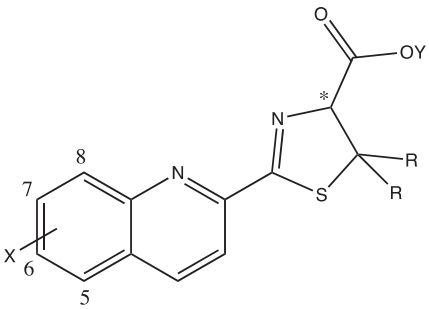


Scheme 1. Outline of the preparation of the benzothiazole SAR-library. The quinoline library was prepared by the same methods. Reagents and conditions: (a) Na₂CO₃ (aq), rt, 3 h; (b) SOCl₂, Methanol, rt, 1 h.

Table 1
Structure and corresponding protein kinase inhibitory activity of compounds **1–16**. Inhibitory activity is expressed as % remaining kinase activity at an inhibitor concentration of 100 μ M.



1 – 12



13 – 16

Compound	X	R	Y	*	DYRK2	DYRK1a	DYRK3	CK2	Aurora A	Aurora B	CDK2/ Cyclin A
1	OH	H	H	S	4	4	5	7	16	6	39
2	OH	H	H	R	9	14	10	41	64	75	43
3	OH	H	CH ₃	S	13	8	30	45	96	91	29
4	OH	H	CH ₃	R	14	9	32	52	42	84	33
5	OCH ₃	H	H	S	31	24	55	84	76	82	92
6	OCH ₃	H	H	R	34	20	55	83	81	106	91
7	OCH ₃	H	CH ₃	S	15	41	15	66	43	83	33
8	OCH ₃	H	CH ₃	R	14	32	18	65	81	85	89
9	OCH ₃	CH ₃	H	S	10	27	21	12	57	109	59
10	OCH ₃	CH ₃	H	R	3	5	4	10	37	99	46
11	OH	CH ₃	H	S	4	4	9	41	58	77	29
12	OH	CH ₃	H	R	1	2	5	21	26	88	12
13	6-OH	H	H	S	4	8	5	9	75	7	64
14	6-OH	H	H	R	17	21	25	34	95	21	66
15	8-OH	H	H	S	5	37	14	14	60	5	45
16	8-OH	H	H	R	27	52	49	52	78	6	45

Dark grey: ≤ 15 , light grey: ≤ 25 .

unaffected by the rest. Furthermore, a few kinases of established drug targeting interest are strongly inhibited by a single member of the library, such as PKB β by compound **10** and PKC ζ by compound **2**. A subset of the full Table (SI), emphasizing the most strongly and broadly inhibited kinases, is reproduced as Table 1 in the main text.

2.3. Structure–activity relationships

Most of the SAR-trends were kinase specific, but masking of the phenol moiety as a methoxy group generally reduced inhibitory

activity compared with the corresponding phenolic compound across the kinase set (with DYRK1a as an exception, being slightly less affected than the other kinases). Esterification of the carboxylate generally reduced inhibitory activity for the phenolic compounds (e.g. compounds **3** and **4** versus compounds **1** and **2**), however for the methoxy-compounds esterification increased activity (e.g. compounds **7** and **8** versus compounds **5** and **6**), in particular for DYRK2 and DYRK3. Introduction of two methyl groups in the dihydrothiazole ring increased inhibitory activity, in particular for the methoxy-compounds, rendering the methoxy-

Table 2Melting temperature (mT) in °C of CDK2 and complexes of CDK2 with inhibitors **1**, **13** and **15**.

Compound	mT	Δ mT	Δ mT (DMSO)
Blank	42.7	0	–
DMSO	41.5	–1.2	0
13	43.4	+0.7	+1.9
15	43.9	+1.2	+2.4
1	47.7	+5	+6.2

gem-dimethyl compounds **9** and **10** almost as effective as their phenolic counterparts **11** and **12**. The stereochemistry of the carboxylate moiety is however more important for the methoxy-compounds **9** and **10**, whereby the *S*-enantiomer **9** is significantly more active than the *R*-enantiomer **10**. This effect is greatly attenuated for the enantiomeric phenols **11** and **12**. Otherwise, stereochemistry seems to play a surprisingly small role for the protein kinases that are promiscuously inhibited by members of the luciferin library. For the protein kinases that are more sensitive to scaffold modifications, such as CK2 and Aurora B, the effect of carboxylate stereochemistry can be significant (e.g. compounds **1** and **2**) or irrelevant (compounds **9** and **10**). There are only minor changes in the kinase inhibition pattern when the 2-benzothiazole-system is exchanged with a 2-quinoline system (e.g. compound **1** versus compound **13**). The effect of carboxylate stereochemistry is however more significant for the 6-hydroxyquinoline derivatives than for corresponding 6-hydroxybenzothiazole derivatives. Moving the hydroxyl-group from the 6-position to the 8-position in the quinoline ring system created more marked changes. The 8-hydroxy-derivatives were generally more active, in particular in relation to DYRK 1a and DYRK3.

Table 3

Data collection and refinement statistics.

Data collection	CDK2/ 1	CDK2/ 15
PDB code	4D1X	4D1Z
Synchrotron radiation	BESSY II	BESSY II
Wavelength, Å	0.9184	0.9184
Number of crystals used	1	1
Number of frames	130	100
Oscillation range/frame	1°	1°
Diffraction data		
Space group	P2 ₁ 2 ₁ 2 ₁	P2 ₁ 2 ₁ 2 ₁
Unit cell parameters, Å	53.31, 72.12, 72.29	53.83, 72.41, 73.06
Protein molecules in asymmetric unit	1	1
Number of measurements	94,018	95,708
Unique reflections	18,036	24,735
Resolution Range, Å (final shell)	50.0–2.1 (2.15–2.10)	50.0–1.85 (1.89–1.85)
Completeness (final shell)	99.7 (98.6)	99.0 (96.7)
I/σ (final shell)	19.62/3.72	15.9/3.4
Merging R factor observed (final shell)	6.7%/46.0%	4.9%/37.8%
Refinement		
Resolution limits, Å (final shell)	42.9–2.1 (2.15–2.10)	30.2–1.85 (1.89–1.85)
Number of used reflections	16,820	22,727
Percentage observed	99.9	99.0
% of free reflections	5.1	5.1
Number of protein atoms	2162	2016
Number of heterogen atoms	18	38
Number of solvent atoms	117	145
R factor overall/free	0.194/0.238	0.195/0.225
Wilson B-factor	28.6 Å ²	25.2 Å ²
RMS bonds/angles	0.004 Å/0.86°	0.005 Å/0.97°
Ramachandran (favored/allowed)	97%/3%	98.4%/1.6%

2.4. Interaction with CDK2

The inhibitory action of D-luciferin on protein kinases was first discovered on CDK2/Cyclin A. Our laboratory has a high throughput screening of kinase structure by soaking on preformed CDK2 crystals, and the initial work and the structural studies were performed on this system.

2.4.1. Thermal shift assay

A thermal shift assay was performed to see whether a binding of D-luciferin (**1**) to CDK2 could be detected by a change in melting temperature. The average thermal shift of the melting temperature was increased by 5 °C for the CDK2 kinase in the presence of D-luciferin. When the benzothiazole ring was replaced by a quinoline ring system as in compounds **13** and **15**, the thermal shift was significantly reduced (Table 2).

2.4.2. X-ray crystal structures of CDK2/inhibitor complexes

To investigate the binding of D-luciferin and its derivatives to CDK2, a set of crystallization experiments were performed. Crystals of apo-CDK2 were soaked with different derivatives and measured at the BESSY II Synchrotron in Berlin. The statistics of the structures are summarized in Table 3. Complexation with compounds **1** and **15** were clearly visible in the electron density maps. Compound **15** had the best fit in the difference density, as seen in Fig. 2. Weaker difference density showed the position of compound **1**, which could be modelled into the map based on the quality of fit to the three strong difference density peaks, attributed to the two sulphur atoms and the hinge binding OH-group. Compound **13** showed unclear density for the fragment in the ATP pocket of CDK2. Compound **13** has only one sulphur atom and the difference density peak for this sulphur atom is weak compared to compound **1**. Inhibitor **13** can still be modelled into the map based on the structure of the CDK2/compound **1** complex, but the CDK2/compound **13** complex is not completely covered by electron density even after refinement. The density map suggests rather that the ATP pocket in this crystal has mixed occupancy, with two partial occupancy water molecules binding to the hinge in addition to the partial occupancy inhibitor.

Compound **1** and **15** bind in different orientations in the ATP pocket of CDK2, as a result that can be attributed to the difference in the OH location in the benzothiazole and quinoline ring systems, respectively. For compound **15**, the shift of the hydroxyl group to the 8-position of the quinoline ring results in a rotation of the inhibitor scaffold by approximately 90° relative to D-luciferin (Figs. 3 and 4), and a different residue in the hinge region is used for hydrogen bonding to the hydroxyl group. Compound **15** creates a hydrogen bond to the carbonyl of the main chain residue L83 (Gatekeeper+3) whereas compound **1** interacts similarly to the carbonyl from residue E81 (Gatekeeper+1). The hydroxyl oxygen atom in both inhibitors accept a hydrogen bond from the amide of L83.

Compound **1** has a length suitable to form an additional hydrogen bond between the carboxylate group and residue T14 in the glycine rich loop. Compound **15** penetrates deeper into the pocket, due to the change in the overall orientation, and therefore does not bind to the glycine rich loop, but makes a hydrogen bond to D145 instead. In Apo CDK2, D145 shares a hydrogen bond with K33 and this H-bond is disrupted by inhibitor **15** binding (Fig. 4).

Compound **1** does not displace this interaction, but instead makes hydrogen bonds with both K33 and D145. A second difference between the binding modes of compound **1** and **15** is the orientation of the dihydrothiazole ring. For compound **1**, the dihydrothiazole sulphur atom is oriented towards the solvent, whereas for compound **15** the dihydrothiazole ring is flipped 180°

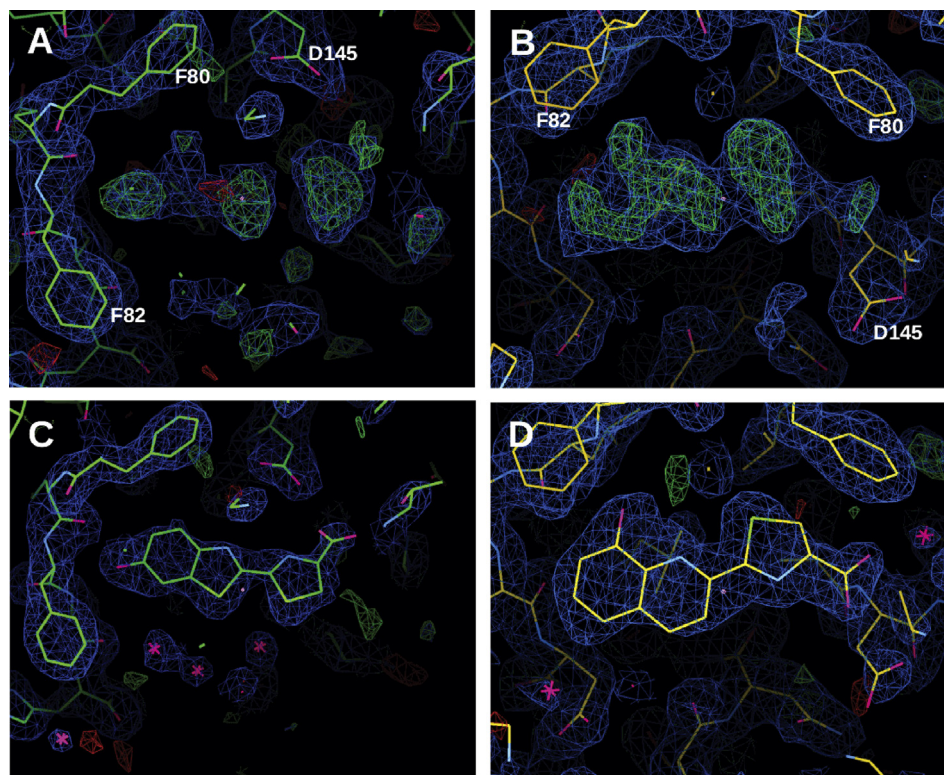


Fig. 2. ATP binding pocket of CDK2. A and B: electron density of the inhibitors before the refinement, and C and D: after the refinement. A and C represents the complex between CDK2 and **1**, whereas B and D represents the complexes with **15**. The electron density is shown in blue at 1σ , the difference density in green and red at 2.5σ for A and B, and at 3σ for C and D.

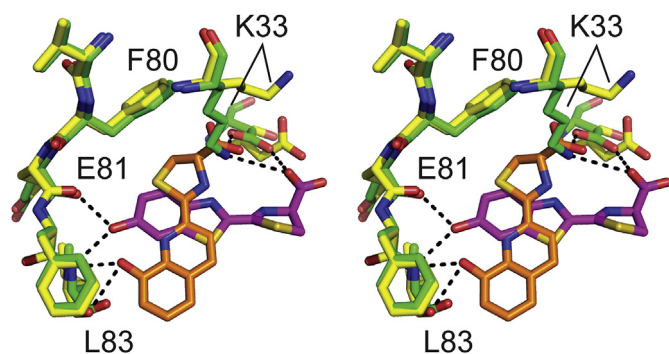


Fig. 3. Orientation of **1** (magenta) and **15** (orange) in the ATP binding pocket of CDK2. Compound **15** is rotated approximately by 90° relative to **1** and penetrates deeper into the ATP pocket. The protein part of CDK2 in complex with **1** is represented in green; with **15** using yellow carbon atoms. The position of the OH group on the benzothiazole and quinoline rings defines the orientation and binding mode of the inhibitor. Both inhibitors bind to the hinge, but use different backbone carbonyl groups for the H-bond.

and the sulphur atom is oriented towards the inside of the ATP pocket (Fig. 3). The presence of weak but significant difference density (Fig. 2, Panel C) adjacent to the sulphur atom in the dihydrothiazole ring of compound **1** might however indicate partial occupancy of the carboxylate also at this position along with an orientation of the dihydrothiazole ring similar to that of **15**. Except for the differences in the binding pocket, the overall structures of the kinase in complexes CDK2/**1** and CDK2/**15** are very similar. In the CDK2/**15** structure however, a second binding site for compound **15** in the C-lobe exists that is not present in the CDK2/**1** structure (Fig. 5).

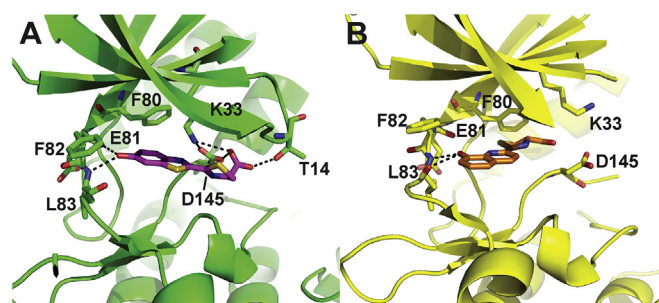


Fig. 4. Binding pocket of CDK2 bound to compounds **1** (A) and **15** (B).

3. Discussion

3.1. Structural interpretation of CDK2-SAR

CDK2/Cyclin A is only modestly inhibited by the compounds of the SAR-library. There are however clear variations in the inhibitory activities for each member in the library due to the change of structural features (Table 1), and most of these trends coincide, albeit at a more attenuated level, with the trends observed for the more strongly inhibited protein kinases. The crystal structures provide insight into key features of binding the luciferin derivatives to CDK2 (Figs. 3 and 4). The general loss of binding efficacy when the methoxy-group replaces the 6-hydroxy group is due to the loss of a hydrogen bond. The phenolic hydroxyl group in D-luciferin (**1**) group anchors the molecule at the kinase hinge segment via two hydrogen bonds: a hydrogen donor interaction to the carbonyl group of E81 (at the Gatekeeper+1 site) with a close O–O distance of 2.8 Å, and a hydrogen acceptor interaction with the amino group

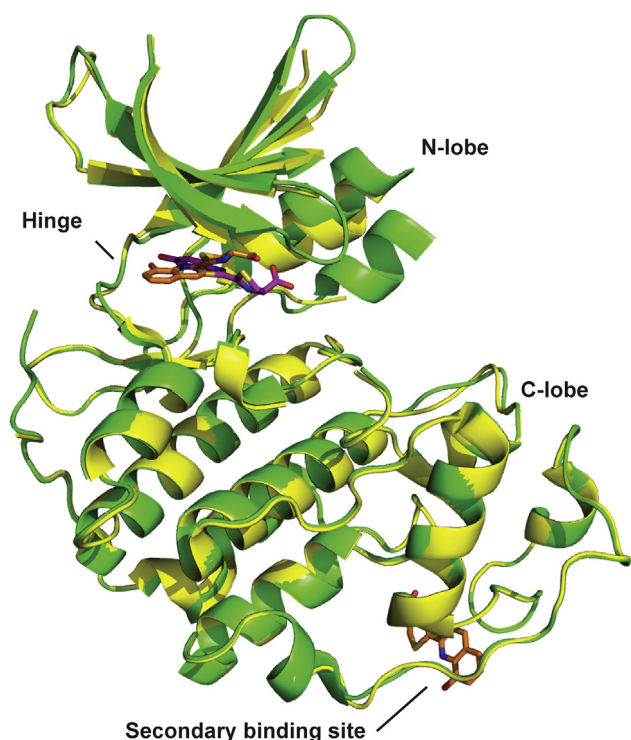


Fig. 5. Superposition of CDK2/1 (green) and CDK2/15 (yellow). The CDK2/15 structure has a secondary binding site for compound **15** in the C-lobe not present in the CDK2/1 structure.

of L83 (Gatekeeper+3), with an O–N distance of 3.0 Å. An identical binding orientation for an inhibitor with a methoxy group substitution (e.g. compound **5**) would not be possible due to steric repulsion from the methyl group. Furthermore, even a displaced methoxy group could function only as a weaker hydrogen bond acceptor [6]. This could explain the weaker binding of compounds **5**, **6**, and **8** compared to compounds **1–4**. However, the exceptional tighter binding of compound **7**, despite the methoxy substitution, requires further studies for clarification. Increase of the lipophilic steric bulk in the dihydrothiazole ring system as in the penicillamine derivatives **9–12** leads to more effective CDK2/Cyclin A inhibitors, a feature that may arise from solvophobic effects introduced by the geminal dimethyl moiety.

On the other hand, the gain in inhibitory efficacy by moving from the carboxylates (e.g. compound **1**) to an ester moiety (e.g. compound **3**) is not trivially explained. In the crystal structure of complex CDK2/1, there is an important interaction between the carboxylate and the salt bridge K33/D145, and it is expected that an esterification of the carboxylate would diminish this interaction. However, the inhibition profile studies are performed not on CDK2 alone, but on the CDK2/Cyclin A complex. Complexation of CDK2 with Cyclin A changes the conformation of the active site of CDK2 in accord with its function as activating cofactor [8,9]. Of particular importance is the movement of helix C (the PSTAIRE-helix) into the catalytic cleft. This movement breaks the salt bridge between K33/D145 and introduces a new salt bridge between K33 and E51 [10]. The carboxylate moiety of D145 will be left exposed to the carboxylate moiety of the luciferin derivatives and create a potential charge clash. This charge repulsion between D145 and the luciferin ligands will be reduced in the carboxylic ester derivatives, and hence explain their higher efficacy as inhibitors.

Based on the understanding of the CDK2 structures and overall SAR data reported here, the SAR features for other individual

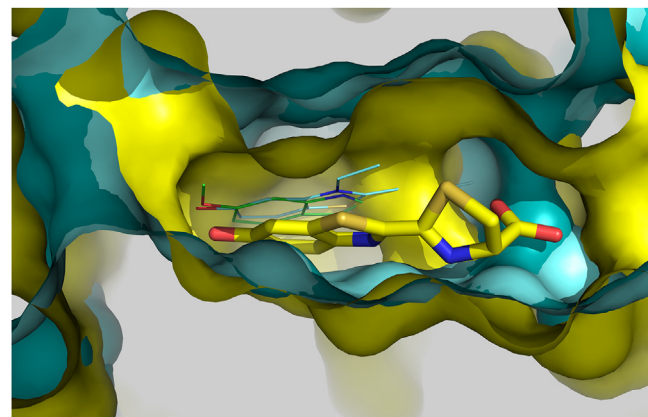


Fig. 6. DYRK1a kinases (3ANR, 3ANQ, cyan) have a differently shaped ATP site in comparison with the CDK2/1 structure (yellow) of this study, due to conformation or rotamer differences in combination with differences in sequence. As a result, luciferin occupies a volume distinct from that of the DYRK inhibitors (see text).

kinases may be analysed based on published structures.

3.2. SAR of DYRK-family inhibition

The members in the DYRK-family of the protein kinases are the most strongly inhibited enzymes by the compounds in the luciferin-library. DYRK2 is the most sensitive kinase in the DYRK-family and will serve as a model for the discussion. DYRK1a and DYRK3 are less affected by the inhibitors, but the inhibition pattern is similar to that of DYRK2, with minor differences. Protein kinases in the DYRK-family are members of the CMGC-kinases, and kinases from other families in the CMGC-group are also significantly inhibited, albeit to a lesser degree, or by fewer members of the library. ERK 8 (a MAP-kinase), CK2 and CDK2 are examples of this.

DYRK2 is promiscuously inhibited by most compounds in the luciferin SAR-library, with only the methoxy carboxylates (compounds **5** and **6**) as inactive inhibitors. Many DYRK-family kinase inhibitors have been reported in the literature (see e.g. Ref. [11] for a recent review). These falls into several diverse molecular frameworks including natural compounds such as β -carboline [3] and acridone [12] alkaloids, flavanols [13], meridianines [14], and lamellarines [15]. Furthermore, synthetic natural product derivatives [16] and fully synthetic molecular scaffolds [17–22] have been developed as kinase inhibitors. Despite this wealth of inhibitor scaffolds, only a few X-ray crystallographic structures of inhibitor/DYRK kinase complexes are available. These include complexes between DYRK1a and the benzothiazole INDY (3ANQ) [23], the β -carboline harmine [23] as well as two pyridopyrimidines (4MQ1 and 4MQ2) [24], and DYRK2 complexes with a bis-indole indigoid (3KVV) [25] or Leucettine L41 (4AZF and 4AZE) [26]. A superposition of published DYRK/inhibitor crystal structures with the CDK2/1 complex (Fig. 6) highlights several features, in particular that the volume of the active site occupied by the inhibitors are distinctly different. As shown in Fig. 6, the inhibitors of the published DYRK1a complex structures interact via a phenolic hydroxy- or a methoxy-group from the inhibitor with the hinge region L241 at the Gatekeeper +3 position [23] in a manner similar to the interaction found in the CDK2/1 complex (*vide supra*). Furthermore, the inhibitors interact through a carbonyl or a pyridine nitrogen with the conserved ATP-binding K188 of DYRK1a in a manner similar to the interaction between the carboxylate of the luciferin inhibitors and K33 of CDK2. Likewise, in the DYRK2 complex with an indigoid inhibitor, similar interactions with the

hinge backbone residues and the conserved lysine are observed. Despite this similarity in interaction sites between the published DYRK complexes and the CDK2/1 complex described here, Fig. 6 clearly shows that the placement and orientation of the DYRK inhibitors differs significantly from **1** in CDK2. This effect can be related to the different shape of the ATP-pocket in the DYRK kinases and CDK2.

The differences in surfaces surrounding the pocket may be attributed to a combination of sequence differences and possibly resultant conformation differences. At the C-lobe side of the binding pocket (in this orientation, at the base), residues isoleucine (DYRK2) and leucine (DYRK1a) restrict the volume relative to alanine of CDK2. Elsewhere at the base of the binding pocket, mutually conserved residues from the C-lobe adopt different rotamers. On the left, differing volumes and conformations of the Gatekeeper +2 residues (phenylalanine and methionine in CDK2 and DYRK1a, respectively) restrict the volume in CDK2. This is linked to a structuring edge-face aromat–aromat interaction between the phenylalanine and the Gatekeeper +4 residue (histidine), which also induces a change in the hinge main chain conformation. Other differences in the shape of the ATP pocket arise from different conformations of the glycine rich loop, which may be due to inhibitor interactions and/or sequence differences; DYRK kinases have a phenylalanine as aromatic residue at the beta hairpin turn of the glycine-rich loop, while CDK2 has a tyrosine. Finally, the binding pockets differ strongly due to positions of the catalytic lysine.

In CDK2, the kinase active site lysine K33 shares a salt bridge interaction with D145, creating the pillar like surface at the rear of the pocket and blocking contact to the gatekeeper phenylalanine. This may be an inhibitor-induced conformation, but seems most likely linked to the absence of a cyclin in the CDK2 structure (*vide supra*). These differences in the shape of the active site of DYRK2 and CDK2 do not offer an obvious explanation for why DYRK2 is more effectively inhibited by members of the luciferin SAR-library than CDK2/Cyclin A.

3.3. SAR of CK2 inhibition

CK2 has been a drug target for well over a decade, and many inhibitors have been identified, one of which has gone to clinical trials [27]. The inhibitors are chemically highly diverse, but many do possess a terminating carboxylic acid group reminiscent of the

inhibitor series we report here. A superposition of these inhibitors using coordinates deposited in the PDB show that the CK2 carboxylate groups form one predominating cluster as salt bridge partners of the active site lysine (Fig. 7). D-luciferin (**1**) and the quinoline cognate **13** both make an analogous interaction in CDK2, hence all effective inhibitors in the SAR series are carboxylates. Furthermore, adding to the importance of the carboxylate for inhibitor binding is the sensitivity for carboxylate stereochemistry, where the *S*-enantiomer is favoured over the *R*-enantiomer. The exception to this pattern is found for the most lipophilic carboxylates (compounds **9** and **10**) where both enantiomers bind equally well.

One distinguishing characteristic of CK2 is its ability to use GTP as the phosphate donor [28], a feature shared with calcium/calmodulin-dependent protein kinase II [29], mst3 kinase [30], protein kinase C δ [31], and relatively few other protein kinases [32]. The structural mechanism by which this occurs in CK2 is that the guanine base, which has a hydrogen bond acceptor–donor–donor pattern (in contrast to adenine's donor–acceptor–empty pattern) binds to the protein kinase hinge slightly shifted in order to align the two acceptor positions. The shift creates a cavity, filled by a water molecule to match the adenine donor position. This anomalous property may be related to the anomalously strong CK2 inhibition of the quinoline derivatives.

3.4. SAR of Aurora A and B inhibition

A significant feature apparent from Table 1 is the inhibition of Aurora B by the quinoline-derived inhibitors **13**, **14**, **15**, and **16**. In contrast, Aurora A is not significantly inhibited by any of these inhibitors, despite its close similarity to Aurora B. This fact may provide key information to identify the mechanisms of selectivity that are operative for the quinoline-derived inhibitors.

The general insensitivity to the position of the hydroxyl substituent suggests that the quinoline inhibitors bind to Aurora B without hinge binding to the hydroxyl group, unlike either of the CDK2 co-crystal structures described above. However, the precise position of the hydroxyl group does affect the sensitivity of Aurora B inhibition to changes in stereochemistry and the relative orientation of the carboxylate group relative to the thiazole ring. For the benzimidazole compounds (**1** vs **2**), there is strong sensitivity to stereochemistry. For the 6-hydroxy quinoline acids (compounds **13** and **14**), the sensitivity is weaker, and for the 8-hydroxy quinoline acids (compounds **15** and **16**) it is absent entirely. These fundamental differences in SAR between CDK2/Cyclin A and the Aurora kinases are not reflected by any obvious differences in the active sites of the proteins, and experimental determination of binding modes in the Aurora kinases seems necessary to understand the origins of the SAR observed for the Aurora kinases.

3.5. Pairwise SAR effects on strongest inhibitors

The exercise of explaining observed inhibitory modulation via pairwise comparisons that focus on individual binding features provides both a test and a summary of SAR hypotheses.

3.5.1. Stereochemistry of the carboxylic acid substituent

As described above, the observed and mostly likely interaction of the carboxylate substituent in the luciferin derivatives is the active site lysine (see also Fig. 7). If this interaction exists in strong inhibitors, as seems likely, changing the stereochemistry would either destroy the interaction and weaken the inhibition, or the interaction would be preserved by a combination of inhibitor rotation, thiazole rotation, and side chain flexibility. A more constrained ATP site and/or binding mode would thus be more

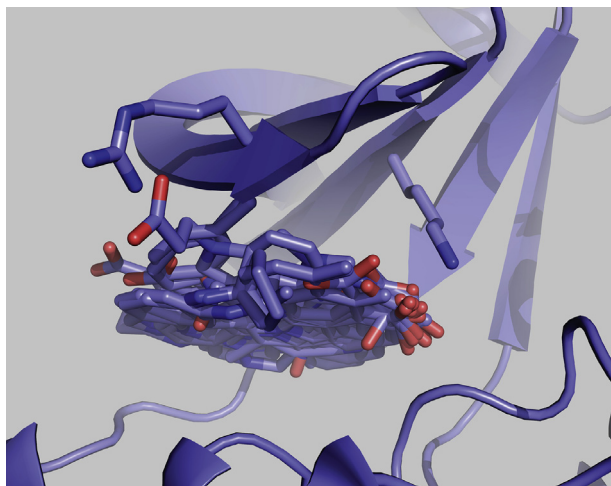


Fig. 7. Carboxylate groups of CK2 inhibitors cluster as salt bridge partners to the active site lysine.

sensitive to the stereochemistry change. Four pairs of inhibitors may be compared to test for these effects. Changing the stereochemistry of D-luciferin (**1**) produces compound **2**, which greatly weakens binding to most kinases strongly inhibited by D-luciferin, however the effect on the DYRK-family is small. The stereochemistry shift between **9** and **10** does not change the strong inhibition of CK2 but stereochemical preference for the DYRK-family changes and now favours the *R*-enantiomer. The corresponding changes between the quinoline enantiomeric pairs of **13/14** and **15/16** show generally similar effects on DYRK 2, DYRK3, CK2, and Aurora B, with the *S*-configuration giving the strongest inhibition.

3.5.2. Neutralization of the carboxylic acid substituent by esterification

If an anionic charge at carboxylate position is important (as we assume for active site lysine salt bridge formation), its neutralization via methylation will show weakened binding. Indeed, this is the case for the two pairs that involve strong inhibition of DYRK2 and DYRK3: **1/3** and **2/4**. DYRK1a is unaffected by this change. However, for the methoxy-compounds **5/7** and **6/8**, the situation is reversed and the more lipophilic ester derivatives are more active than the free acids.

3.5.3. Modification of lipophilic bulk

The addition of methyl groups to the dihydrothiazole ring are seen with pairs **1/11**, **2/12**, **5/9**, and **6/10**. The addition of bulk to luciferin (**1/11**) is fully tolerated by the strongly inhibited kinases in the DYRK-family. The other strongly inhibited kinases loose activity upon methylation of the dihydrothiazole ring. The enantiomeric **2/12** with *R*-configuration at the carboxylate pair shows that methylation even increases inhibition of the DYRK-kinases. For the methoxylated pairs **5/9** and **6/10** differing only by the stereochemistry of the carboxylate on the dihydrothiazole, methylation is tolerated by the DYRK-kinases while the CK2-kinase is substantially more inhibited.

3.5.4. Modifications of the benzothiazole or quinoline phenol

Methylation of the benzothiazole phenol eliminates strong binding when compared to the phenolic benzothiazoles, except for **9** and **10** inhibition of CK2 and DYRK2. This is consistent with most binding modes involving hydrogen bonding of the alcohol to the hinge. Unique characteristics of CK2 and DYRK2 have been discussed above and include GTP binding to CK2 and the generally strong inhibition of DYRK2 by all compounds. The methoxy derivatives require a carboxylic acid for CK2 inhibition. In striking contrast to benzothiazoles, the quinolines inhibit only Aurora B, CK2 and DYRK2 strongly, as discussed above. Binding patterns for these three proteins are qualitatively similar.

4. Conclusion

The observation that D-luciferin inhibits quite selectively several protein kinases in the CMGC-group has two important consequences. First, D-luciferin and cognates represent a useful fragment-like scaffold for protein kinase inhibitor design with an interesting intrinsic selectivity for the DYRK-family of protein kinases complementing the already known molecular scaffolds. Furthermore, the profiling and SAR analysis here also demonstrate good potential for achieving a wide range of selectivity patterns among the other drug target kinases described here. With multiple binding geometries at the hinge, and multiple positions for further derivatisation, the scaffolds provide myriad possibilities for drug design. On the other hand, the multiple binding geometries limits the extension of the qualitative understanding of the SAR derived from the structures of CDK2 complexes to other kinases.

Second, the potential for ligand interactions to be shared between protein kinases and luciferases deserves close attention, as luciferin/luciferase based assays are in widespread use. Awareness of this possibility may aid interpretation of apparently anomalous results.

5. Experimental

5.1. Protein expression, purification and crystallization

CDK2 was expressed with an N-terminal His-tag in BL21(DE3) cells. The protein was purified via a His-tag column (50 mM sodium phosphate, 500 mM NaCl, pH 7.0) and eluted via an imidazole gradient (50 mM sodium phosphate, 300 mM NaCl, 500 mM imidazole pH 7.0). The combined fractions with the CDK2 were loaded on an S200 16/60 gel filtration column (10 mM Hepes, 20 mM NaCl, 2 mM DTT, pH 7.4). CDK2 formed crystals spontaneously after concentrating the fractions from the gel filtration above 6 mg/ml at 4 °C.

5.2. Structure determination

Crystals were soaked with either D-luciferin or the derivatives and cryoprotected with glycerol prior to the freezing. The crystals were measured at the Berlin Electron Storage Ring Society for Synchrotron Radiation (BESSY II) in Berlin/Germany.

5.3. Thermal shift assay

20 µL of CDK2 wild-type protein 0.7–0.8 mg/ml (50 mM phosphate buffer pH 7.5, 150 mM NaCl) was mixed with 5 µL 6% SyproOrange (Sigma). 1 µL of DMSO or 1 µL of 10 mM inhibitor dissolved in DMSO was added. The thermal shift assay was done on a Miniopticom (Biorad) by heating the sample slowly from 20 °C to 90 °C with a step interval of 1/3 °C. All experiments were performed in triplicate.

5.4. Preparation of inhibitors

The inhibitors were prepared by a condensation between cysteine and a benzothiazole nitrile or a quinoline nitrile derivative. Demethylation of the aromatic methoxy group or esterification of the dihydrothiazolecarboxylate group was preformed as needed. ¹H NMR and ESI mass spectral data for all compounds were in accordance with the literature and are given in the Supplementary Information.

5.5. Determination of protein kinase inhibition

The determination of protein kinase inhibition was performed at the International Centre for Kinase Profiling at the University of Dundee, U.K. The method used is a radioactive filter binding assay using 33P ATP [3,33]. The ATP concentrations were at or below the calculated K_m for ATP for each particular kinase.

Acknowledgement

Provision of beam time at Bessy II, Berlin Germany at BL14.1 is gratefully acknowledged. Special thanks to the Helmholtz center, for supporting the travel expenses for Ulli Rothweiler.

Appendix A. Supplementary data

Supplementary data related to this article can be found at <http://dx.doi.org/10.1016/j.ejmech.2015.02.035>.

References

- [1] A. Lundin, J. Eriksson, A real-time bioluminescent HTS method for measuring protein kinase activity influenced neither by ATP concentration nor by luciferase inhibition, *Assay Drug Dev. Technol.* 6 (2008) 531–541.
- [2] P. Singh, B.J. Harden, B.J. Lillywhite, P.M. Broad, Identification of kinase inhibitors by an ATP depletion method, *Assay Drug Dev. Technol.* 2 (2004) 161–169.
- [3] J. Bain, L. Plater, M. Elliott, N. Shapiro, C.J. Hastie, H. McLauchlan, I. Klevernic, J.S. Arthur, D.R. Alessi, P. Cohen, The selectivity of protein kinase inhibitors: a further update, *Biochem. J.* 408 (2007) 297–315.
- [4] E.H. White, F. McCapra, G.F. Field, The structure and synthesis of firefly luciferin, *J. Am. Chem. Soc.* 85 (1963) 337–343.
- [5] D.C. McCutcheon, M.A. Paley, R.C. Steinhardt, J.A. Prescher, Expedient synthesis of electronically modified luciferins for bioluminescence imaging, *J. Am. Chem. Soc.* 134 (2012) 7604–7607.
- [6] G. Meroni, M. Rajabi, E. Santaniello, D-Luciferin, derivatives and analogues: synthesis and in vitro/in vivo luciferase-catalyzed bioluminescent activity, *ARKIVOC* 2009 (2009) 265–288.
- [7] H.-J. Böhm, S. Brode, U. Hesse, G. Klebe, Oxygen and nitrogen in competitive situations: which is the hydrogen-bond acceptor? *Chem. A Eur. J.* 2 (1996) 1509–1513.
- [8] P.D. Jeffrey, A.A. Russo, K. Polyak, E. Gibbs, J. Hurwitz, J. Massague, N.P. Pavletich, Mechanism of CDK activation revealed by the structure of a cyclinA-CDK2 complex, *Nature* 376 (1995) 313–320.
- [9] A.A. Russo, P.D. Jeffrey, A.K. Patten, J. Massague, N.P. Pavletich, Crystal structure of the p27Kip1 cyclin-dependent-kinase inhibitor bound to the cyclin A-Cdk2 complex, *Nature* 382 (1996) 325–331.
- [10] R.A. Engh, D. Bossemeyer, The protein kinase activity modulation sites: mechanisms for cellular regulation – targets for therapeutic intervention, *Adv. Enzyme Regul.* 41 (2001) 121–149.
- [11] B. Smith, F. Medda, V. Gokhale, T. Dunckley, C. Hulme, Recent advances in the design, synthesis, and biological evaluation of selective DYRK1A inhibitors: a new avenue for a disease modifying treatment of Alzheimer's? *ACS Chem. Neurosci.* 3 (2012) 857–872.
- [12] M.A. Beniddir, E. Le Borgne, B.I. Iorga, N. Loac, O. Lozach, L. Meijer, K. Awang, M. Litaudon, Acridone alkaloids from *Glycosmis chlorosperma* as DYRK1A inhibitors, *J. Nat. Prod.* 77 (2014) 1117–1122.
- [13] J. Bain, H. McLauchlan, M. Elliott, P. Cohen, The specificities of protein kinase inhibitors: an update, *Biochem. J.* 371 (2003) 199–204.
- [14] M. Gompel, M. Leost, E.B. De Kier Joffe, L. Puricelli, L.H. Franco, J. Palermo, L. Meijer, Meridianins, a new family of protein kinase inhibitors isolated from the ascidian *Aplidium meridianum*, *Bioorg. Med. Chem. Lett.* 14 (2004) 1703–1707.
- [15] C. Neaogio, E. Vedrenne, F. Buron, J.Y. Merour, S. Rosca, S. Bourg, O. Lozach, L. Meijer, B. Baldeyrou, A. Lansiaux, S. Routier, Synthesis of chromeno[3,4-b]indoles as Lamellarin D analogues: a novel DYRK1A inhibitor class, *Eur. J. Med. Chem.* 49 (2012) 379–396.
- [16] M. Debdab, F. Carreaux, S. Renault, M. Soundararajan, O. Fedorov, P. Filippakopoulos, O. Lozach, L. Babault, T. Tahtouh, B. Baratte, Y. Ogawa, M. Hagiwara, A. Eisenreich, U. Rauch, S. Knapp, L. Meijer, J.P. Bazureau, Leucettines, a class of potent inhibitors of cdc2-like kinases and dual specificity, tyrosine phosphorylation regulated kinases derived from the marine sponge leucettamine B: modulation of alternative pre-RNA splicing, *J. Med. Chem.* 54 (2011) 4172–4186.
- [17] P. Kassis, J. Brzeszcz, V. Beneteau, O. Lozach, L. Meijer, R. Le Guevel, C. Guillouzo, K. Lewinski, S. Bourg, L. Colliandre, S. Routier, J.Y. Merour, Synthesis and biological evaluation of new 3-(6-hydroxyindol-2-yl)-5-(phenyl)pyridine or pyrazine V-shaped molecules as kinase inhibitors and cytotoxic agents, *Eur. J. Med. Chem.* 46 (2011) 5416–5434.
- [18] Y. Loidreau, P. Marchand, C. Dubouilh-Benard, M.R. Nourrisson, M. Duflos, O. Lozach, N. Loac, L. Meijer, T. Besson, Synthesis and biological evaluation of N-arylbenzo[b]thieno[3,2-d]pyrimidin-4-amines and their pyrido and pyrazino analogues as Ser/Thr kinase inhibitors, *Eur. J. Med. Chem.* 58 (2012) 171–183.
- [19] Y. Loidreau, P. Marchand, C. Dubouilh-Benard, M.R. Nourrisson, M. Duflos, N. Loac, L. Meijer, T. Besson, Synthesis and biological evaluation of N-aryl-7-methoxybenzo[b]furo[3,2-d]pyrimidin-4-amines and their N-arylbenzo[b]thieno[3,2-d]pyrimidin-4-amine analogues as dual inhibitors of CLK1 and DYRK1A kinases, *Eur. J. Med. Chem.* 59 (2013) 283–295.
- [20] L. Demange, F.N. Abdellah, O. Lozach, Y. Ferandin, N. Gresh, L. Meijer, H. Galons, Potent inhibitors of CDK5 derived from roscovitine: synthesis, biological evaluation and molecular modelling, *Bioorg. Med. Chem. Lett.* 23 (2013) 125–131.
- [21] E. Deau, Y. Loidreau, P. Marchand, M.R. Nourrisson, N. Loac, L. Meijer, V. Levacher, T. Besson, Synthesis of novel 7-substituted pyrido[2',3':4,5]furo[3,2-d]pyrimidin-4-amines and their N-aryl analogues and evaluation of their inhibitory activity against Ser/Thr kinases, *Bioorg. Med. Chem. Lett.* 23 (2013) 6784–6788.
- [22] O. Dehbi, A. Tikad, S. Bourg, P. Bonnet, O. Lozach, L. Meijer, M. Aadil, M. Akssira, G. Guillaumet, S. Routier, Synthesis and optimization of an original V-shaped collection of 4-7-disubstituted pyrido[3,2-d]pyrimidines as CDK5 and DYRK1A inhibitors, *Eur. J. Med. Chem.* 80 (2014) 352–363.
- [23] Y. Ogawa, Y. Nonaka, T. Goto, E. Ohnishi, T. Hiramatsu, I. Kii, M. Yoshida, T. Ikura, H. Onogi, H. Shibuya, T. Hosoya, N. Ito, M. Hagiwara, Development of a novel selective inhibitor of the down syndrome-related kinase Dyrk1A, *Nat. Commun.* 1 (2010) 86.
- [24] K. Anderson, Y. Chen, Z. Chen, R. Dominique, K. Glenn, Y. He, C. Janson, K.C. Luk, C. Lukacs, A. Polonskaia, Q. Qiao, A. Railkar, P. Rossman, H. Sun, Q. Xiang, M. Vilenchik, P. Wovkulich, X. Zhang, Pyrido[2,3-d]pyrimidines: discovery and preliminary SAR of a novel series of DYRK1B and DYRK1A inhibitors, *Bioorg. Med. Chem. Lett.* 23 (2013) 6610–6615.
- [25] M. Soundararajan, A.K. Roos, P. Savitsky, P. Filippakopoulos, A.N. Kettenbach, J.V. Olsen, S.A. Gerber, J. Eswaran, S. Knapp, J.M. Elkins, Structures of down syndrome kinases, DYRKs, reveal mechanisms of kinase activation and substrate recognition, *Structure* 21 (2013) 986–996.
- [26] T. Tahtouh, J.M. Elkins, P. Filippakopoulos, M. Soundararajan, G. Burgy, E. Durieu, C. Cochet, R.S. Schmid, D.C. Lo, F. Delhommel, A.E. Oberholzer, L.H. Pearl, F. Carreaux, J.P. Bazureau, S. Knapp, L. Meijer, Selectivity, cocrystal structures, and neuroprotective properties of leucettines, a family of protein kinase inhibitors derived from the marine sponge alkaloid leucettamine B, *J. Med. Chem.* 55 (2012) 9312–9330.
- [27] G. Cozza, L.A. Pinna, A. Moro, Protein kinase CK2 inhibitors: a patent review, *Expert Opin. Ther. Pat.* 22 (2012) 1081–1097.
- [28] K. Niefind, M. Putter, B. Guerra, O.G. Issinger, D. Schomburg, GTP plus water mimic ATP in the active site of protein kinase CK2, *Nat. Struct. Biol.* 6 (1999) 1100–1103.
- [29] S.L. Bostrom, J. Dore, L.C. Griffith, CaMKII uses GTP as a phosphate donor for both substrate and autophosphorylation, *Biochem. Biophys. Res. Commun.* 390 (2009) 1154–1159.
- [30] K. Schinkmann, J. Blenis, Cloning and characterization of a human STE20-like protein kinase with unusual cofactor requirements, *J. Biol. Chem.* 272 (1997) 28695–28703.
- [31] M. Gschwendt, W. Kittstein, K. Kielbassa, F. Marks, Protein-kinase C-Delta accepts Gtp for autophosphorylation, *Biochem. Biophys. Res. Commun.* 206 (1995) 614–620.
- [32] C.A. Smith, M. Toth, H. Frase, L.J. Byrnes, S.B. Vakulenko, Aminoglycoside 2'-phosphotransferase IIIa (APH(2')-IIIa) prefers GTP over ATP: structural templates for nucleotide recognition in the bacterial aminoglycoside-2' kinases, *J. Biol. Chem.* 287 (2012) 12893–12903.
- [33] C.J. Hastie, H.J. McLauchlan, P. Cohen, Assay of protein kinases using radio-labeled ATP: a protocol, *Nat. Protoc.* 1 (2006) 968–971.